Catalysis Today 170 (2011) 64–68

Contents lists available at ScienceDirect

Catalysis Today

journal homepage: www.elsevier.com/locate/cattod

Dehydrogenation of ammonia borane catalyzed by in situ synthesized Fe–Co nano-alloy in aqueous solution

F.Y. Qiu, Y.J. Wang*, Y.P. Wang, L. Li, G. Liu, C. Yan, L.F. Jiao, H.T. Yuan

Institute of New Energy Material Chemistry, Key Laboratory of Advanced Energy Materials Chemistry (MOE) Nankai University, Tianjin 300071, PR China

ARTICLE INFO

Article history:
Received 31 October 2010
Received in revised form 21 February 2011
Accepted 22 February 2011
Available online 2 April 2011

Keywords:
$Fe_{1-x}Co_x$ alloys
Catalysts
In situ synthesized
Hydrolysis
Ammonia borane
Hydrogen generation

ABSTRACT

In this paper, a series of $Fe_{1-x}Co_x$ alloys ($x = 0, 0.3, 0.5, 0.6, 0.7, 1$) is in situ synthesized by a chemical reduction method and used as catalysts for generating hydrogen from aqueous solution of ammonia borane (NH_3BH_3) at room temperature. XRD and TEM characterizations reveal that these $Fe_{1-x}Co_x$ nano-alloys are amorphous and ultrafine. The hydrogen generation measurements show that in situ synthesized $Fe_{1-x}Co_x$ alloys exhibit excellent catalytic properties. The hydrogen generation rate of $Fe_{0.3}Co_{0.7}$ alloy can reach to the maximum of 8945.5 ml min^{-1} g^{-1} at 293 K and the activation energy is only 16.30 kJ mol^{-1}. Furthermore, the hydrolysis of NH_3BH_3 is completed within 1.8 min. The results are better than Fe, Co nano-particles and ex situ synthesized samples, which could be attributed to electron transfer from Fe to active Co sites, and improvement in the dispersion of the catalyst with Fe_2O_3.

1. Introduction

In the past few years, the energy crisis and greenhouse gas emissions have seriously affected political and environmental climates [1]. Great efforts have been paid for the development of new energy system, which is one of the most important research fields in chemistry, biology and material science. Among lots of new energy materials, high-capacity hydrogen storage materials have been paid more and more attention because of their friendliness towards the environment [2]. Currently, great interest has been shown in developing high performance hydrogen storage materials for on-board applications. Ammonia borane (NH_3BH_3) is a promising material for future energy program for its high hydrogen storage capacity, light weight and stabilization of its solution at room temperature [3–11]. The hydrolysis of ammonia borane can be represented as follows [11]

$$NH_3BH_3 + 2H_2O \rightarrow NH_4^+ + BO_2^- + 3H_2\uparrow$$

However, the hydrolysis rate of ammonia borane is very low without any catalyst. In this sense, selecting a suitable catalyst becomes the main issue. Traditionally, noble metals such as Ru [12–16], Pt [11,12], Pd [11,16] and Rh [11,12,17,18] show preferable activities in hydrogen generation from ammonia borane, while their use in practical applications is limited for their high cost. Thus, some low-cost catalysts have been revealed, such as solid acid [19] and transition metals. Among them, transition metals such as Fe, Co, Ni [20–25], have been paid more and more attention. And their catalytic activities are closely related to the particle sizes. Yan et al. [20] reported that in situ prepared Fe nano-particle possessed better catalytic property for the hydrolysis of ammonia borane, comparing with ex situ synthesized Fe sample. However, the catalytic activity of Fe nano-particle for the dehydrogenation of ammonia borane is still very low. Meanwhile, bimetallic nano-alloys such as Pt–Ni [26], Fe–Ni [21], Au–Ni [27], Au–Co [28] alloys exhibit better catalytic activities than single metal for hydrogen generation from the hydrolysis of ammonia borane, which is attributed to the synergy effect between two kinds of metals. Thus, we tried to in situ synthesize $Fe_{1-x}Co_x$ alloys in order to improve the hydrolysis rate of ammonia borane.

In this work, a series of $Fe_{1-x}Co_x$ nano-alloys ($x = 0, 0.3, 0.5, 0.6, 0.7, 1$) was in situ synthesized by chemical reduction and applied as catalysts for the dehydrogenation of ammonia borane. The optimal $Fe_{1-x}Co_x$ alloys and the corresponding activation energy were studied.

2. Experimental

2.1. In situ synthesized $Fe_{1-x}Co_x$ nano-alloys and their catalytic properties for the hydrolysis of Ammonia borane

$Fe_{1-x}Co_x$ ($x = 0$, 0.3, 0.5, 0.6, 0.7, 1) nano-alloys were prepared by a simple in situ synthesis method [20,21]. $NaBH_4$ (Sodium borohydride, Alfa Aesar, 97%) is the reductant. The

* Corresponding author. Tel.: +86 22 23503639; fax: +86 22 23503639.
E-mail address: wangyj@nankai.edu.cn (Y.J. Wang).

0920-5861/$ – see front matter © 2011 Elsevier B.V. All rights reserved.
doi:10.1016/j.cattod.2011.02.026

products with different molar ratios (χ_{Co}) were obtained by varying the concentration of Co and Fe salts in initial solution (NH_3BH_3:($FeSO_4$ + $CoCl_2$):$NaBH_4$ = 1.0:0.12:0.17). The molar ratio for ($FeSO_4$ + $CoCl_2$):$NaBH_4$) was kept a constant of 1:1.4 [22,29]. Typically, a mixture of $NaBH_4$ (11 mg) and NH_3BH_3 (ammonia borane, Sigma–Aldrich, 90%) (55 mg) was kept in a sealed flask fitted with an outlet tube for collecting evolved hydrogen gas. Chloride hexahydrate ($CoCl_2{\cdot}6H_2O$, Alfa Aesar, 98.0–102.0%) and iron(II) sulfate heptahydrate ($FeSO_4{\cdot}7H_2O$, Tian Jin Guang Fu Technology Development Co., Ltd. >99%) with varying proportions were dissolved in 10 ml distilled water to make an uniformly mixed solution, which was then rapidly dropped into the flask with vigorous stirring at controlled temperature. The volume of generated H_2 was monitored by water displacement method.

When the hydrolysis reaction was completed, $Fe_{1-x}Co_x$ (x = 0, 0.3, 0.5, 0.6, 0.7, 1) catalysts were washed and filtered three times with distilled water and ethanol absolute under Ar atmosphere. After dried in vacuum at 333 K for 4 h, the samples were collected for tests. The ex situ sample was prepared in the same conditions as in the in situ synthesized samples, except the absence of ammonia borane.

2.2. Catalyst characterization

The in situ synthesized $Fe_{1-x}Co_x$ nano-alloys were characterized by X-ray diffraction (XRD, Rigaku D/max-2500, Cu Kα radiation), where a glass substrate holding the powder sample was covered by an adhesive tape on the surface to prevent the sample from exposure to air, and transmission electron microscope (TEM, Philips Tecnai G^2 F20 equipped with an energy dispersive X-ray spectrometer (EDX) for elemental analysis). Surface electronic states and valence state were carried out by X-ray photoelectron spectroscopy (XPS, Kratos Axis Ultra DLD multi-technique).

3. Results and discussion

Fig. 1 shows the hydrogen generation volume as the function of reaction time obtained by the hydrolysis of ammonia borane catalyzed by in situ synthesized $Fe_{1-x}Co_x$ (x = 0, 0.3, 0.5, 0.6, 0.7, 1) alloys and ex situ synthesized $Fe_{0.3}Co_{0.7}$ alloy at 293 K. The first 10 s, accompanied by H_2 release, the black $Fe_{1-x}Co_x$ particles were rapidly generated. All of the nano-alloys exhibit excellent catalytic activities (Fig. 1), which is better than the catalytic activity of pure

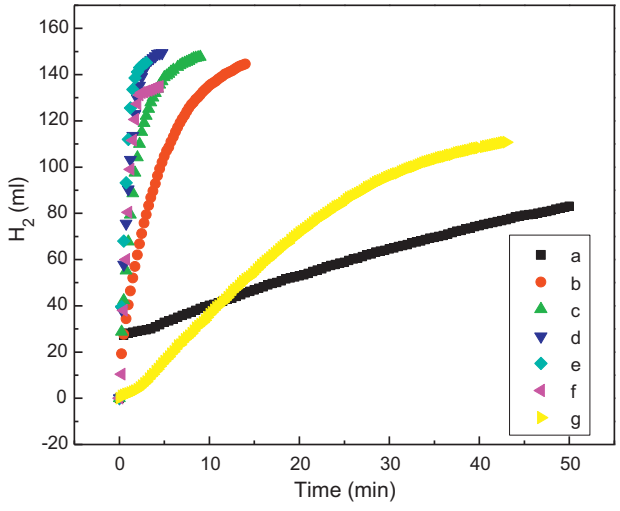

Fig. 1. Hydrogen generation from the hydrolysis of ammonia borane in the presence of (a–f) in situ synthesized $Fe_{1-x}Co_x$ alloys (x = 0, 0.3, 0.5, 0.6, 0.7, 1) and (g) ex situ synthesized $Fe_{0.3}Co_{0.7}$ alloy at 293 K.

Table 1
The max hydrogen generation rate for the hydrolysis of ammonia borane catalyzed by in situ synthesized $Fe_{1-x}Co_x$ alloys (x = 0, 0.3, 0.5, 0.6, 0.7, 1) and ex situ synthesized $Fe_{0.3}Co_{0.7}$ alloy (ex situ-$Fe_{0.3}Co_{0.7}$) at 293 K.

Catalysts	The max. hydrogen generation rate (ml min^{-1} g^{-1})
Fe	114.5
$Fe_{0.7}Co_{0.3}$	3170.6
$Fe_{0.5}Co_{0.5}$	5463.3
$Fe_{0.4}Co_{0.6}$	7877.1
$Fe_{0.3}Co_{0.7}$	8945.5
Co	7437.9
Ex situ-$Fe_{0.3}Co_{0.7}$	348.3

Co and Fe for the hydrolysis of ammonia borane. Otherwise, increasing with the Co content (x), the hydrolysis rate increases at first and then decreases slightly (a–f in Fig. 1). Among them, $Fe_{0.3}Co_{0.7}$ alloy displays the best catalytic performance, delivering a high hydrogen release rate of 8945.53 ml min^{-1} g^{-1} at 293 K and complete reaction time of 1.8 min. The molar ratio of hydrolytically generated H2 to the initial NH3BH3 is close to 3.0, indicating that the hydrolysis reaction is completed. Meanwhile, the hydrolysis rate of ammonia borane catalyzed by in situ prepared Fe is the slowest, only half amount of the H2 release in 30 min. The corre-

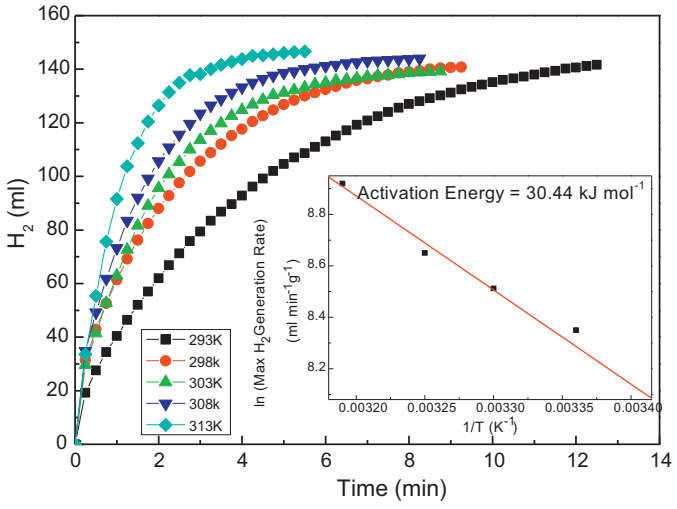

Fig. 2. Hydrogen generation from the hydrolysis of ammonia borane in the presence of in situ synthesized $Fe_{0.7}Co_{0.3}$ alloy at different temperatures.

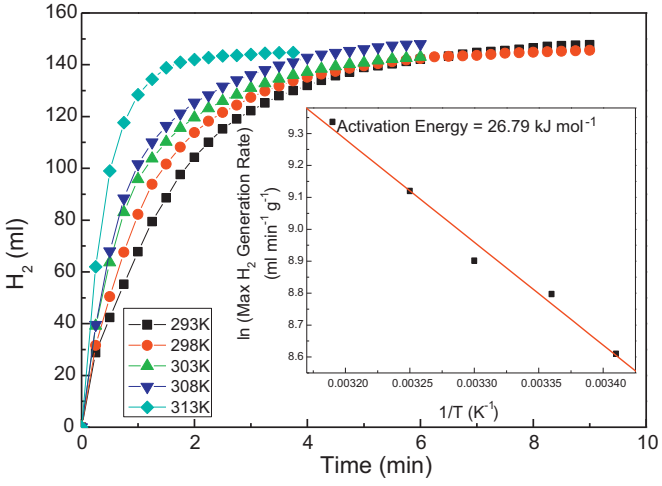

Fig. 3. Hydrogen generation from the hydrolysis of ammonia borane in the presence of in situ synthesized $Fe_{0.5}$ $Co_{0.5}$ alloy at different temperatures.

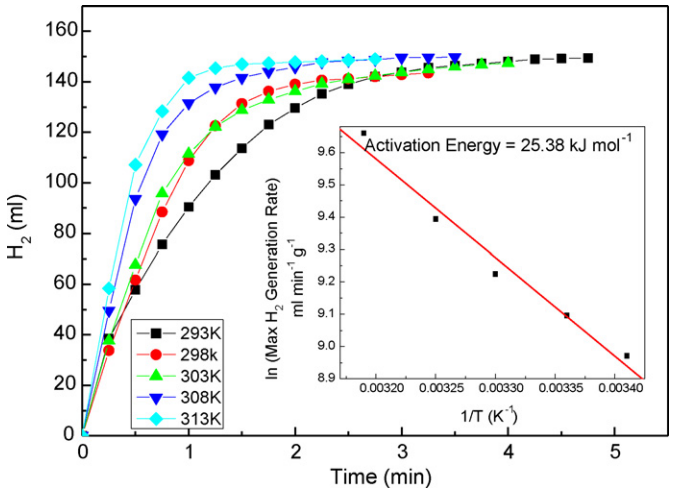

Fig. 4. Hydrogen generation from the hydrolysis of ammonia borane in the presence of in situ synthesized $Fe_{0.4}Co_{0.6}$ alloy at different temperatures.

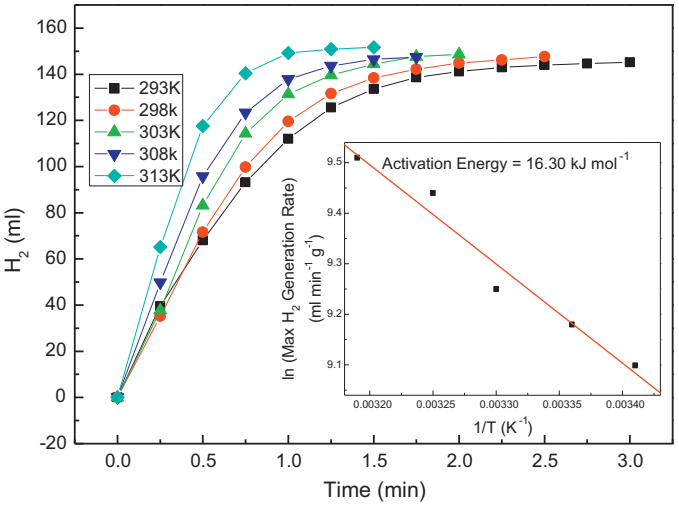

Fig. 5. Hydrogen generation from the hydrolysis of ammonia borane in the presence of in situ synthesized $Fe_{0.3}Co_{0.7}$ alloy at different temperatures.

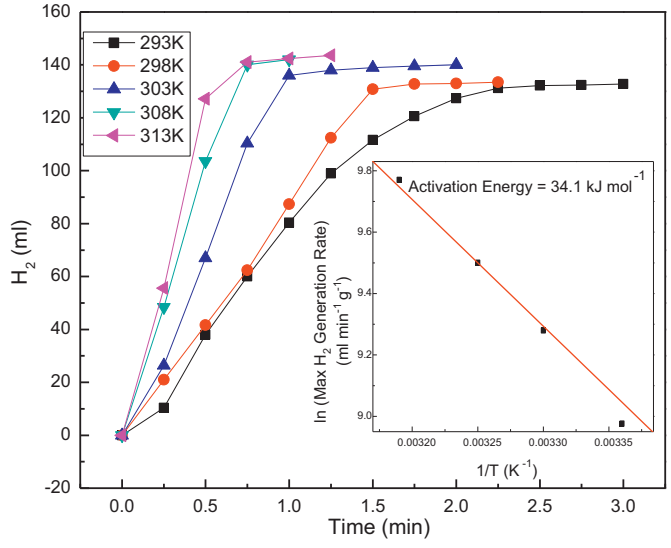

Fig. 6. Hydrogen generation from the hydrolysis of ammonia borane in the presence of in situ synthesized Co at different temperatures.

Table 2
The max hydrogen generation rate for the hydrolysis of ammonia borane catalyzed by in situ synthesized $Fe_{1-x}Co_x$ alloys (x = 0, 0.3, 0.5, 0.6, 0.7, 1) at different temperatures.

Temperature (°C)	The max. hydrogen generation rate (ml min^{-1} g^{-1}) with different catalysts in situ synthesized				
	$Fe_{0.7}Co_{0.3}$	$Fe_{0.5}Co_{0.5}$	$Fe_{0.4}Co_{0.6}$	$Fe_{0.3}Co_{0.7}$	Co
20	3170.6	5463.3	7877.1	8945.5	7437.9
25	4147.8	6616.6	8921.7	9716.3	7909
30	4976.1	7344.6	10146.2	12208.6	10742.5
35	5712.2	9147.0	12016.6	12561.2	13295.6
40	7477.9	11339.4	12753.2	13438.8	17508

sponding maximum hydrogen generation rates (R_{max}) are shown in Table 1. R_{max} obtained by in situ synthesized Fe nano-particle is 114.5 ml min^{-1} g^{-1} at 293 K, suggesting that Fe has inferior catalytic activity for the hydrolysis of ammonia borane. The optimum R_{max} of ammonia borane catalyzed by in situ synthesized $Fe_{0.3}Co_{0.7}$ alloy is 8945.5 ml min^{-1} g^{-1} at 293 K, which is much better than that of the ex synthesized $Fe_{0.3}Co_{0.7}$ alloy.

In order to study the effects of the temperature on the hydrogen generation rate, a series of experiments was operated at different solution temperatures, ranging from 293 K to 313 K by using in situ synthesized $Fe_{1-x}Co_x$ alloys (x = 0.3, 0.5, 0.6, 0.7, 1) (Figs. 2–6). The maximum hydrogen generation rates at different temperatures are

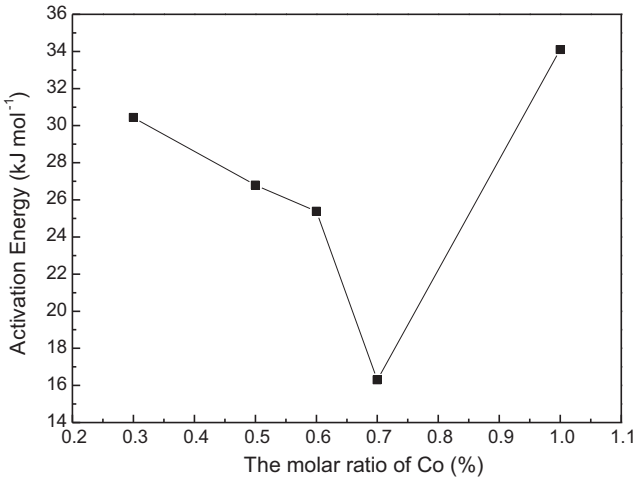

Fig. 7. The relationship of activation energy and the content of Co in $Fe_{1-x}Co_x$ alloys (x = 0.3, 0.5, 0.6, 0.7, 1).

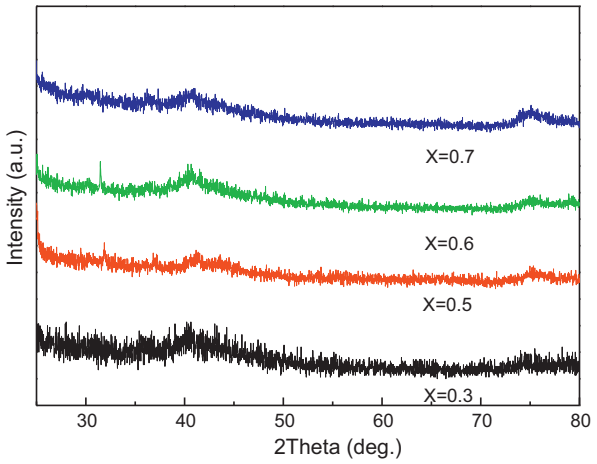

Fig. 8. XRD patterns of in situ synthesized $Fe_{1-x}Co_x$ alloys (x = 0.3, 0.5, 0.6, 0.7).

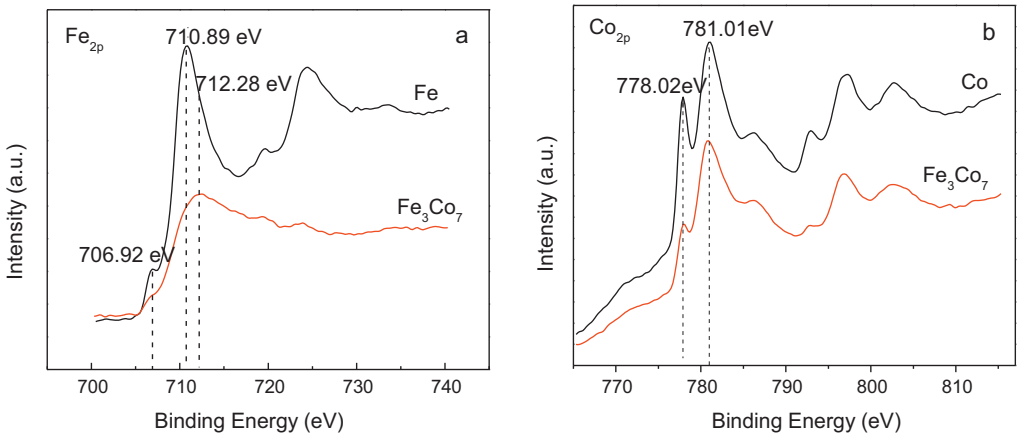

Fig. 9. XPS Spectra of (a) Fe 2p and (b) Co 2p level for in situ synthesized Fe, $Fe_{0.3}Co_{0.7}$ and Co catalysts.

shown in Table 2. The relationship of the activation energy and the content of Co(x) is illustrated in Fig. 7. In the beginning, it decreases with the growing content of Co(x) in the $Fe_{1-x}Co_x$ alloys (x = 0.3, 0.5, 0.6, 0.7), and then increases sharply. The activation energy of $Fe_{0.3}Co_{0.7}$ alloy shows 16.30 kJ mol^{-1}. This is much lower than the previous report [26].

Fig. 8 shows the XRD patterns of the in situ synthesized $Fe_{1-x}Co_x$ alloys (x = 0.3, 0.5, 0.6, 0.7). All the catalysts show similar diffraction patterns, demonstrating the amorphous forms of the samples. Two broad peaks are found at about $2\theta = 41^\circ$ and 76°, respectively. As compared to that of pure Co, there is little shift for the diffraction peaks, manifesting the substitution of the Fe atoms for the Co atoms in $Fe_{1-x}Co_x$ alloys. It is also confirmed by XPS test.

XPS spectra of Fe, $Fe_{0.3}Co_{0.7}$, Co catalysts are presented in Fig. 9. Two peaks with the binding energy (BE) of 778.02 and 781.01 eV are observed for $Co_{2p2/3}$ level in Co and $Fe_{0.3}Co_{0.7}$ catalysts, which

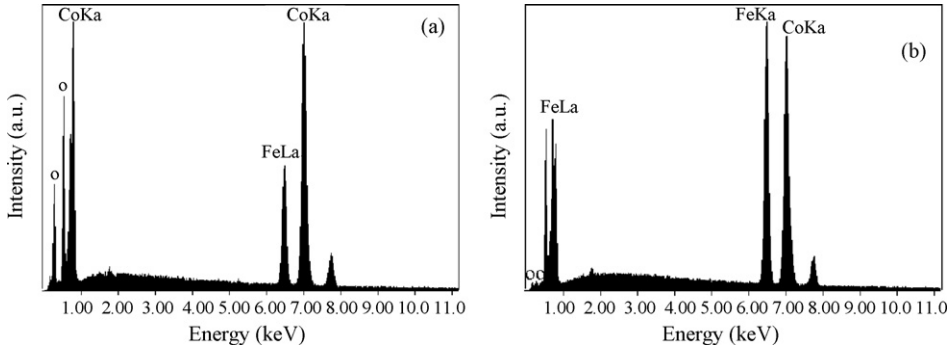

Fig. 10. EDX spectra of $Fe_{1-x}Co_x$ nano-particles: (a) $Fe_{0.3}Co_{0.7}$ and (b) $Fe_{0.5}Co_{0.5}$.

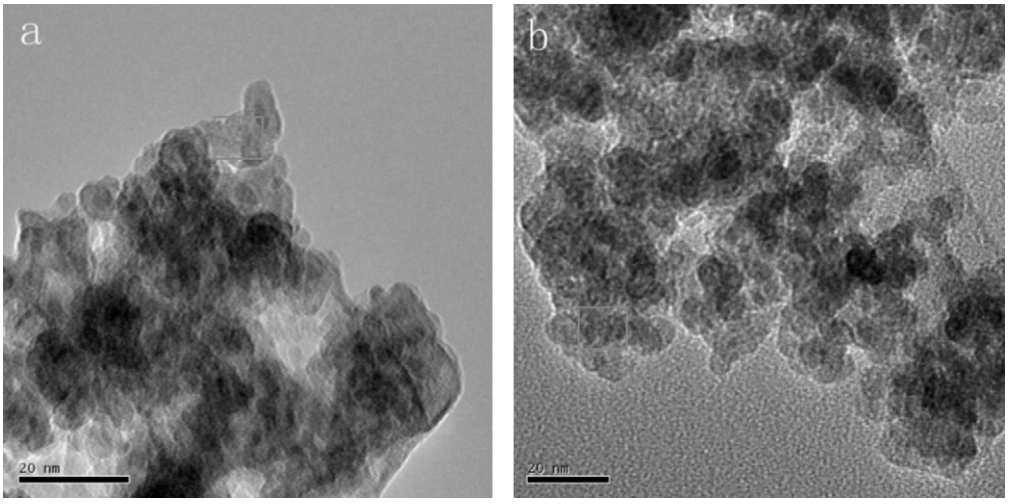

Fig. 11. TEM images of in situ synthesized (a) $Fe_{0.3}Co_{0.7}$ alloy and (b) $Fe_{0.5}Co_{0.5}$ alloy.

are attributed to elemental and oxidized Co, respectively. The peak assigned to oxidized Co is mainly related to $Co(OH)_2$, which would have been formed during the reaction owning to the alkaline solution [30]. Two peaks are also gained for the $Fe_{2p2/3}$ level in Fe catalyst, indicating that Fe exists in both the elemental and oxidized states. However, for Fe catalyst, the peak of elemental iron is very weak. What is more, is the BE value of the oxidized iron in Fe catalyst is higher than that of $Fe_{0.3}Co_{0.7}$ catalyst, which is related to the electron transfer from Fe to Co. Therefore, metallic Co is enriched with the electron while Fe is electron deficient in $Fe_{0.3}Co_{0.7}$ catalyst. The electron deficient Fe is strongly adsorbed on electron-enriched Co active sites, which repels the adsorption of oxygen atoms. Fig. 10 shows the EDX spectra of $Fe_{1-x}Co_x$ catalysts ($x = 0.5$, 0.7), which were taken from the specially marked areas in the TEM images. The EDX data (Fig. 10a) of $Fe_{0.3}Co_{0.7}$ catalyst confirms average elemental composition of the alloy. It shows that the molar ratio of Fe and Co is very close to 3:7, which is consistent with the XPS analysis that oxygen atoms are repelled by the absorbed Fe in $Fe_{0.3}Co_{0.7}$ catalyst. Similarly, a typical EDX image of $Fe_{0.5}Co_{0.5}$ catalyst is also achieved (Fig. 10b). The molar ratio of Fe and Co extremely agrees with the original proportion (5:5). In other words, Fe effectively protects Co from oxidation [31,32]. However, the content of oxygen atoms in $Fe_{0.3}Co_{0.7}$ catalyst is a little higher than that of $Fe_{0.5}Co_{0.5}$ catalyst, which may attribute to the formation of Fe_2O_3.

In addition, aggregation can be found from the typical TEM images of $Fe_{1-x}Co_x$ alloys ($x = 0.7$, 0.5) (Fig. 11). This may be attributed to the magnetic property of these alloys. However, the average particle sizes of the prepared catalysts are less than 10 nm, which is relative to the formation of Fe_2O_3 according to the XPS results. Fe_2O_3 formed in the reaction can play the role of dispersion, not only relieving the aggregation of the particles but also resulting in more Co active sites in the catalytic reaction [33,34]. Therefore, the activity of $Fe_{0.3}Co_{0.7}$ catalyst is higher than other catalysts prepared in this work.

4. Conclusions

In summary, $Fe_{1-x}Co_x$ alloys ($x = 0$, 0.3, 0.5, 0.6, 0.7, 1) are successfully in situ synthesized by chemical reduction at room temperature. $Fe_{0.3}Co_{0.7}$ displays an excellent catalytic activity for the hydrolysis of ammonia borane solution. It has the maximum hydrogen generation rate of 8945.5 ml min^{-1} g^{-1} at 293 K and low activation energy of 16.30 kJ mol^{-1}. The enhanced hydrogen generation rate, lower activation energy and costs indicate that $Fe_{1-x}Co_x$ alloys may have potential applications for the hydrolysis of ammonia borane.

Acknowledgement

This work was financially supported by MOST projects (2010CB631303), NSFC (50971071, 51071087) and MOE (IRT-0927).

References

[1] J.M. Yan, X.B. Zhang, S. Han, H. Shioyama, Q. Xu, Inorg. Chem. 48 (2009) 7389–7393.
[2] Ö. Metin, S. Özkar, Energy Fuels 23 (2009) 3517–3526.
[3] Q. Xu, M. Chandra, J. Power Sources 163 (2006) 364–370.
[4] S.B. Kalidindi, M. Indirani, B.R. Jagirdar, Inorg. Chem. 47 (2008) 7424–7429.
[5] M. Rakap, S. Özkar, Int. J. Hydrogen Energy 35 (2010) 3341–3346.
[6] M. Rakap, S. Özkar, Int. J. Hydrogen Energy 35 (2010) 1305–1312.
[7] M. Diwan, D. Hanna, A. Varma, Int. J. Hydrogen Energy 35 (2010) 577–584.
[8] B. Peng, J. Chen, Energy Environ. Sci. 1 (2008) 479–483.
[9] T. Umegaki, J.M. Yan, X.B. Zhang, H. Shioyama, N. Kuriyama, Q. Xu, Int. J. Hydrogen Energy 34 (2009) 2303–2311.
[10] H.L. Jiang, S.K. Singh, J.M. Yan, X.B. Zhang, Q. Xu, ChemSusChem 3 (2010) 541–549.
[11] M. Chandra, Q. Xu, J. Power Sources 156 (2006) 190–194.
[12] Q. Xu, M. Chandra, J. Alloys Compd. (2007) 729–732, 446–447.
[13] F. Durap, M. Zahmakıran, S. Özkar, Int. J. Hydrogen Energy 34 (2009) 7223–7230.
[14] S. Basu, A. Brockman, P. Gagare, Y. Zheng, P.V. Ramachandran, W.N. Delgass, J.P. Gore, J. Power Sources 188 (2009) 238–243.
[15] S.C. Amendola, S.L. Sharp-Goldman, M.S. Janjua, N.C. Spencer, M.T. Kelly, P.J. Petillo, M. Binder, Int. J. Hydrogen Energy 25 (2000) 969–975.
[16] Ö. Metin, Ş. Şahin, S. Özkar, Int. J. Hydrogen Energy 34 (2009) 6304–6313.
[17] S. Çalışkan, M. Zahmakıran, S. Özkar, Appl. Catal. B 93 (2010) 387–394.
[18] F. Durap, M. Zahmakıran, S. Özkar, Appl. Catal. A 369 (2009) 53–59.
[19] M. Chandra, Q. Xu, J. Power Sources 159 (2006) 855–860.
[20] J.M. Yan, X.B. Zhang, S. Han, H. Shioyama, Q. Xu, Angew. Chem. Int. Ed. 47 (2008) 2287–2289.
[21] J.M. Yan, X.B. Zhang, S. Han, H. Shioyama, Q. Xu, J. Power Sources 194 (2009) 478–481.
[22] J.M. Yan, X.B. Zhang, H. Shioyama, Q. Xu, J. Power Sources 195 (2010) 1091–1094.
[23] Y. Yamada, K. Yano, Q. Xu, S. Fukuzumi, J. Phys. Chem. 114 (2010) 16456–16462.
[24] T. Umegaki, J.M. Yan, X.B. Zhang, H. Shioyama, N. Kuriyama, Q. Xu, J. Power Sources 191 (2009) 209–216.
[25] T. Umegaki, J.M. Yan, X.B. Zhang, H. Shioyama, N. Kuriyama, Q. Xu, Int. J. Hydrogen Energy 34 (2009) 3816–3822.
[26] X.J. Yang, F.Y. Cheng, J. Liang, Z.L. Tao, J. Chen, Int. J. Hydrogen Energy 34 (2009) 8785–8791.
[27] H.L. Jiang, T. Umegaki, T. Akita, X.B. Zhang, M. Haruta, Q. Xu, Chem. Eur. J. 16 (2010) 3132–3137.
[28] J.M. Yan, X.B. Zhang, T. Akita, M. Haruta, Q. Xu, J. Am. Chem. Soc. 132 (2010) 5326–5327.
[29] Y.P. Wang, Y.J. Wang, Q.L. Ren, L. Li, L.F. Jiao, D.W. Song, G. Liu, Fuel Cells 10 (2010) 132–138.
[30] W.L. Dai, M.H. Qiao, J.F. Deng, Appl. Surf. Sci. 120 (1997) 119–124.
[31] R. Fernandes, N. Patel, A. Miotello, M. Filippi, J. Mol. Catal. A: Chem. 298 (2009) 1–6.
[32] H. Li, Y. Wu, H. Luo, M. Wang, Y. Xu, J. Catal. 214 (2003) 15–25.
[33] E. Leclercq, A. Rives, E. Payen, R. Hubaut, Appl. Catal. A 168 (1998) 279–288.
[34] A. Yokoyama, H. Komiyama, H. Inoue, T. Masumoto, H.M. Kimura, J. Catal. 68 (1981) 355–361.